# MODELLING OF EVOLUTION OF TRANSFER PROPERTIES DUE TO EXPANSION OF CONCRETE INDUCED BY INTERNAL SWELLING REACTION

Yuichiro Kawabata[1, 2*], Renaud-Pierre Martin[1], Jean-François Seignol[1], François Toutlemonde[1],

[1] Université Paris-Est, IFSTTAR, Materials and Structures Department, Marne-la-Vallée, FRANCE

[2] Port and Airport Research Institute, Structural Engineering Division, Yokosuka, JAPAN

**Abstract**

This paper presents a coupling model between expansion due to internal swelling reactions (ISR) and evolution of transfer properties. The coupling model was devised based on previous experiments and then trial calculations were performed. According to the trial calculations with simplified conditions, the simulated results with coupling showed quite different behaviour from the ones without coupling. The results emphasized the importance of taking into account the evolution of transfer properties due to ISR expansion to obtain more reliable prediction of concrete structures affected.

**Keywords**: internal swelling reaction, transfer properties, couplings, moisture state

## 1 INTRODUCTION

Internal swelling reactions (ISR) such as alkali-silica reaction (ASR) and delayed ettringite formation (DEF) induce cracks and decrease mechanical properties of concrete. The structures subjected to ISR may raise some serious issues of concrete in terms of serviceability. Severe deteriorations lead to loss of operability and/or safety, resulting in replacement/reconstruction of the concrete member or structure. In real structures, because of moisture gradients within structures and between structures and external environments, moisture transfers can take place. ISR-induced expansion is so sensitive to humidity that wet parts of the structure show expansion as opposed to drying parts that may even shrink. It is important, therefore, to evaluate precisely the moisture state within the structure.

There are three main mechanisms for moisture transfer: diffusion due to concentration gradient, permeation due to flow of fluids under a pressure gradient and sorption by capillary suction. Previous studies evidenced that expansion due to ISR induces microcracks and the microcracks increase transfer properties of concrete, resulting in strain variation within the structures [1-4]. Martin et al. claimed that the evolution of transfer properties and coupling between expansion and transfer properties should be taken into consideration in the predictive models [1], otherwise the calculation underestimates the expansion because less moisture imbibition would be predicted.

This paper firstly presents a literature review regarding the effects of cracking and ISR expansion on transfer properties. Then, despite the fact that few data is available for evolution of transfer properties, the modeling approach is introduced. Finally, trial simulations on simplified cases and boundary conditions are presented.

## 2 LITERATURE REVIEW

### 2.1 Cracking effect on the evolution of transfer properties

The effect of width of a single crack on diffusivity has been investigated in numerous papers, especially focusing on chloride ion penetration. When the damage is at the microcracking level, it has little effect on chloride ion diffusivity while it has significant effect when crack width reaches approximately 75 - 80 μm [5-7]. Sorptivity is also affected by microcracks. Sahmaran and Li reported that the sorptivity of Engineered Cementitious Composites (ECC) is increased by microcracks induced by mechanical loading [8]. Water permeability increases with increase in crack width exponentially [9-11]. Some papers indicated "threshold effect": the permeability is not increased by the existence of crack up to a certain width [10, 12]. But recent papers claimed that such phenomenon cannot be observed and this effect is attributable to the measurement method of crack width [13].

* Correspondence to: kawabata-y@pari.go.jp

Recent work by Wu et al. [14], focusing on the effect of drying-induced microcracks on the transfer properties, clarified that the gas permeability and water sorptivity are less sensitive to micro-cracking. This result suggests that the influence of cracking is different according to moisture transfer mechanism.

### 2.2 Effect of ISR expansion

Due to the complex and badly known influence of water (either liquid or vapor) and ions on ISR development, less information is available for evolution of transfer properties due to ISR. ISR induces multidirectional microcracks so that the effect of crack would be more complicated. According to Al Shamaa et al. [3-4], the permeability of concrete due to DEF increases up to 70 times when the concrete expands up to 0.7 % with respect to non-expanded concrete (Figure 1). The comparison between numerical analysis and experiments revealed that this effect is lower in the case of lower expansion (ASR: 0.3 %) [15] though it is significant in the case of larger expansion such as in case of DEF [1]. The experiments by Al Shamaa et al., however, revealed that the permeability increases up to 20 times when expansion exceeds 0.27 % [3]. The experiments by Al Shamaa were performed on non-loaded concrete. Actual concrete structures are subjected to mechanical loading so that the damage induced by ISR is not isotropic. Anisotropic damage would influence the anisotropic transfer properties in concrete. No data has been available for transfer properties of concrete with anisotropic damage. In addition, the first author revealed that the effect of water precipitation on the ASR expansion of field-exposed concrete block becomes more significant when expansion of concrete block is over 0.04 %, according to the numerical simulation [16]. This 0.04 % of expansion almost corresponds to the criteria adopted in the EU PARTNER project for surface cracking of concrete blocks [17]. Surface cracking makes ingress of liquid water easier so that the inner concrete core is maintained under wet conditions. This result indicates that the evolution of transfer properties may be more significant in field conditions where concrete structures are subjected to direct supply of liquid water.

## 3 MODELLING APPROACH

Although the effect of microcracks induced by ISR on transfer properties still needs documented experimental evidences, it is important to implement the evolution of transfer properties in the predictive models for ISR. Here, we devised a simple model for evolution of transfer properties with respect to ISR expansion and performed trial calculations. The models related to the trial calculation are also described below.

### 3.1 ISR expansion

ISR-induced expansion can be formulated according to equation (1). This equation consists in the product of swelling potential by a kinetics term [1].

$$\varepsilon_\chi = \varepsilon_\infty \xi(t) \tag{1}$$

where, the strain tensor $\varepsilon_\infty$ is ultimate expansion, representative of swelling potential, $\xi(t)$ is the kinetics part which expresses the degree of reaction which evolves from 0, at the beginning of reaction, to 1, at the end of reaction.
The kinetic term can be described with four parameters, following equation (2) [18-19].

$$\xi(t) = \frac{1-\exp\left(-t/\tau_c\right)}{1+\exp\left(-\frac{t-\tau_l}{\tau_c}\right)} \begin{cases} 1 & \text{for ASR} \\ \left(1-\frac{\phi}{\delta+t}\right) \text{ with } 0 \le \phi < \delta & \text{for DEF} \end{cases} \tag{2}$$

where, $t$ is elapsed time, $\tau_c$ and $\tau_l$ are characteristic and latency times, respectively. $\phi$ and $\delta$ are corrective parameters.

### 3.2 Moisture effect

Three parameters, $\varepsilon_\infty$, $\tau_c$ and $\tau_l$, are moisture-dependent parameters. In further calculations, the saturation degree, $s$, was used as the relevant descriptor of moisture content of the material [15]. The moisture-dependency can be expressed according to the following equations, with a reference to Poyet [20-21].

$$\varepsilon_{\infty}(s)=\varepsilon_{\infty}(100\%)\left(\frac{\langle s-s_{\infty\_\varepsilon_{\infty}}\rangle^{+}}{1-s_{\infty\_\varepsilon_{\infty}}}\right)^{m_{\varepsilon_{\infty}}} \quad (3)$$

$$\tau_{c,l}(s)=\tau_{c,l}(100\%)\Big/\left(\frac{\langle s-s_{\infty\_\tau_{c,l}}\rangle^{+}}{1-s_{\infty\_\tau_{c,l}}}\right)^{m_{\tau_{c,l}}} \quad (4)$$

where, $s_{\infty\_x}$ is threshold saturation degree of parameter $x$ below which no expansion occurs. $m_x$ is nonlinearity parameter of $x$.

### 3.3 Moisture diffusion

Moisture diffusion can be calculated solving the following differential equation (5):

$$\frac{\partial s}{\partial t}-D_s\cdot\frac{\partial s^2}{\partial^2 x}=0 \quad (5)$$

where, $D_s$ is the diffusion coefficient and s is the saturation degree.
Moisture transport shows nonlinearity depending on humidity or saturation degree of pores. Here, the nonlinear diffusion model proposed by Bazant and Najjar was applied [22].

$$D_s = D_0\left(\alpha_0+\frac{1-\alpha_0}{1+\left(\frac{1-s}{1-s_c}\right)^n}\right) \quad (6)$$

where, $D_0$, $a_0$, $n$ and $s_c$ are experimental material constants.

### 3.4 Evolution of moisture transfer properties

Advancement of ISR induces microcracks of concrete, resulting in new paths for diffusion of moisture. Although the effect of these microcracks on the evolution of diffusion coefficient remains not clear, the evolution of transfer properties would relate to the damage so that the conventional damage model was applied to the evolution of diffusion coefficient [23].

$$D_{s,\varepsilon}/D_{s,0}= 1+d_{max}\{1-\exp(-\omega\langle\varepsilon_t-\varepsilon_{cr}\rangle^{+})\} \quad (7)$$

where, $D_{s,0}$ is the diffusion coefficient of non-expanded concrete, $d_{max}$ and $\omega$ are materials parameters representing maximum value for evolution and rate of damage evolution, respectively. $\varepsilon_{cr}$ is the threshold expansion above which diffusion coefficient starts increasing.

### 3.5 Shrinkage

The shrinkage is basically formulated as linearly varying with moisture content and can be written following Eq. (8) [24-25].

$$\varepsilon_{sh}(t)=k_{sh}(s_{(t)}-s_{ini}) \quad (8)$$

where, $k_{sh}$ is shrinkage coefficient, $s_{(t)}$ and $s_{ini}$ are saturation degree at time $t$ and initial state, respectively.

## 4 TRIAL CALCULATIONS

The models described above have been integrated in a calculation system set up using MATLAB software. In order to grasp the effect of evolution of transfer properties on ISR expansion, 1-D calculations as case study were performed. The details are described in the following. Parameters used are shown in Table 1. Fifteen cases were performed in this study, as summarized in Table 2.

### 4.1 Parameter settings

ASR expansion was simulated with Eqs. (1) and (2). The ultimate expansion was set to be 1.0 %, which is usually intermediate value between ASR and DEF. Latency and characteristic times were set for concrete to expand rapidly in the calculation. For moisture effect, $s_{\infty}$ and $m$ were set to be 0.8 and 1.0, respectively, as reasonable values for ASR expansion. The parameters for nonlinear moisture diffusion were set to be almost the same as in reference [22]. $k_{sh}$ for shrinkage is derived from reference [2].

It is well known that the mechanism of moisture diffusion is quite different from that of gas permeation. Since no data regarding the influence of expansion on the moisture diffusivity have been available, the assumption was made that the influence of ISR expansion on the diffusivity is the same

as that on permeability as a first step. Based on this assumption, $d_{max}$, $\omega$ and $\varepsilon_{cr}$ are set to be 100, 1 and 0.04 %, respectively as standard values, with reference to the experimental data as shown in the regression curve of Figure 1. The calibrated model is also illustrated in Figure 1. Because few experimental data has been available up to now, other values were also tested for sensitivity analysis (see Table 1 and Figure 2). The significance of the parameters regarding the evolution can be clearly observed in Figures 1-2. It should be noted that further experimental investigation would be necessary to quantify these parameters.

Initial saturation degree is one of the key parameters for moisture diffusion and start of ISR expansion. In this study, 0.8 was adopted as a standard (Table 2).

### 4.2 Boundary conditions

A long concrete specimen (500 mm) in which lateral surface has been kept sealed and the end surface with different boundary conditions is considered. One end surface is exposed to constant humid condition (saturation degree = 0.8) whilst the other end surface is subjected to three types of boundary conditions: they are shown in Figure 3. This situation has been designed as an idealized 1-D gradient corresponding to Multon's and Martin's experiments (500 mm-deep beams under moisture gradient) [2, 15].

### 4.3 Calculation algorithm

The algorithm for calculation is shown in Figure 4. At first time step, because of no expansion, diffusion coefficient can be calculated with the saturation degree. Then the moisture field is calculated with Eqs. (5) - (6). According to the saturation degree of moisture in each element, the incremental expansion is calculated. Likewise, at time step $t$, diffusion coefficient is updated by Eq. (7), with accordance to expansion up to time $t$-1. Then the moisture field and resultant expansion is calculated. Time step was set to be 0.005 day and the calculation was looped over time up to 1000 days.

Here, since the asymptotic final expansion depends on the saturation degree, chemical reaction advancement is clearly different when the saturation degree changes. Therefore the corresponding time to have the same expansion as that of the different saturation degree should be calculated (Figure 5). At time step $t_i$, the virtual time $vt_{i-1}$, at which the master curve of expansion calculated with the parameters at time step $t_i$ is equal to that at time step $t_{i-1}$ ($\varepsilon_{i-1}$), is calculated. Then the incremental expansion at $vt_i$ ($vt_{ti} = vt_{i-1} + \Delta t$) is calculated by substituting the calibrated parameters according to the actual saturation degree in the rate form of Equation (2). Finally expansion at time $t_i$ ($\varepsilon_i$) is calculated by adding calculated incremental expansion ($\Delta\varepsilon_i$) to the former expansion ($\varepsilon_i = \varepsilon_{i-1} + \Delta\varepsilon_i$).

Shrinkage is also considered in Cases 12-15. The total strain is calculated by adding shrinkage strain to the chemical strain.

## 5 RESULTS AND DISCUSSIONS

### 5.1 Effect of boundary conditions

The simulated responses in terms of expansion and saturation degree of concrete with different boundary conditions are shown in Figure 6. Each graph comprises expansion curves, corresponding to strain/saturation degree at different depth from the surface, taking into account the coupling between expansion and moisture transfer properties, or not. In Figure 6 (a), in which the boundary condition is constant wetting, the expansion behaviour at 10 mm is almost the same, regardless of whether evolution of transfer properties is implemented or not. At 100mm and 200mm, however, kinetics of expansion is accelerated by the transfer evolution. In the cases with Model B, expansions seem to reach a plateau. For the expansions of the cases with Model A the evolution model catches up with the implemented cases but after a longer duration. For this boundary condition, both end sides are fixed so that it is reasonable that the simulated expansion with Model A catches up with the one with implementation. It should be noted that, at 200 mm from the lower surface, maximum rate of expansion of concrete with Model B is more than two times larger than that without implementation. Thus the calculation with Model A underestimates the expansion of inner concrete.

In Figure 6 (b), in which the boundary condition is stepwise wetting, the surface response (10 mm) is almost the same, irrespective of implementation of the evolution model. The important point is that the saturation degree of the inner part is significantly increased in the case of Model B. This effect is very clear at 100 mm after about 800 days. Simultaneously expansion of concrete is also accelerated by moisture imbibitions. Therefore, once the concrete structure is affected by ISR, the change in moisture condition has a critical impact on the prediction of expansion behaviour, especially during wetting process, which is consistent with field experience [16, 26].

The results above are focused on wetting process but the drying process is also important for the prediction. The simulated results for wetting/drying as boundary condition are illustrated in Figure 6 (c). In this case, the part near the surface is also crucial for expansion. At 10 mm from the surface, the expansion of the case with Model B at 1000 days is 1.5 times larger than the one without implementation. It can also be pointed out that the expansion with Model A at 10 mm almost reaches a plateau whereas the case with Model B shows continuous expansion. This tendency can also be observed at 100 mm. The mechanism can be explained with the difference of saturation degree. In the absence of transfer evolution, the peak of each wave profile is almost stabilized after the second or third peak. Consequently the expansion tends to reach a plateau up to the asymptotic final expansion associated to this saturation degree. On the contrary the peak of the case with Model B becomes gradually higher at each cycle. The evolution of transfer properties induces larger variations of saturation degree so that the concrete shows complicated behaviour and simultaneous expansion.

### 5.2 Effect of calibration of the model accounting for coupling between expansion and transfer properties

Figure 7 shows the expansion profiles at different timesteps with different threshold expansion values to take into account the transfer evolution, $\varepsilon_{cr}$. The results are quite reasonable: the lower the threshold, the larger the expansion. The expansion response with 0.5 % as threshold is almost similar to the case with Model A. Therefore, in order to grasp the effect of threshold on ISR expansion clearly, the relationship between threshold and expansion at 300 mm from the surface is summarized in Figure 8. After 600 days, the differences between different threshold values can be clearly distinguished and should be determined using appropriate experimental data. Yet, experimental data regarding the relationship between expansion and moisture transfer properties are limited.

The effect of damage rate, $\omega$ values, on ISR expansion was also investigated. The simulated expansions at 50 mm with different $\omega$ values and boundary conditions are illustrated in Figure 9. In the cases except for wetting/drying condition, the effect of $\omega$ values on expansive behaviour can hardly be observed only in the cases of variable hydraulic boundary conditions. It turned out that ISR expansion is not sensitive to $\omega$ in the conditions set in this study. From these results, threshold expansion, $\varepsilon_{cr}$, is the most sensitive parameter compared to the rate of evolution, $\omega$.

## 6 CONCLUDING REMARKS

A coupling model between chemical expansion and transfer properties was presented based on previous experiments and trial calculations were performed. Trial calculations revealed that, with implementation of the model for evolution of transfer properties, the predicted results were quite different. In the case in which the evolution model is implemented, inner part of concrete starts expansion earlier. When the concrete is subjected to wetting/drying, the evolution affects not only the expansion of inner part but also the one of surface part. The results emphasized the importance of accounting for evolution of transfer properties due to ISR expansion for more reliable prediction of concrete structures affected by ISR expansion. Further works on experiments and simulations are necessary to refine the model.

For the future works, the authors are planning to carry out the basic experiments modelled in this paper to verify the model described above. The calculation of the deformation of large-scale beams tested by Multon [15, 27] and the second author [1, 2] will be also planned.

## 7 REFERENCES


[1] Martin, R.-P.: Experimental analysis of the mechanical effects of delayed ettringite formation on concrete structures. PhD thesis. Université Paris Est. 2010 (in French).

[2] Martin, R.-P., Omikrine-Metalssi, O. and Toutlemonde, F.: Importance of considering the coupling between transfer properties, alkali leaching and expansion in the modelling of concrete beams affected by internal swelling reactions, Const. Build. Mat., Vol. 49 pp. 23-30, 2013.

[3] Al Shamaa, M. et al.: Coupling between mechanical and transfer properties and expansion due to DEF in a concrete of a nuclear power plant, Nuc. Eng., Vol. 266, pp. 70-77, 2014.

[4] Al Shamaa, M. et al.: Influence of relative humidity on delayed ettringite formation, Cem. Con. Comp., Vol. 58, pp. 14-22, 2015.

[5] Kato, E., Kato, Y. and Uomoto, T.: Development of simulation model of chloride ion transportation in cracked concrete, J. Adv. Concr. Tech., Vol. 3, pp. 85-94, 2005.

[6] Djerbi, A. et al.: Influence of traversing crack on chloride diffusion into concrete, Cem. Con. Res., Vol. 38, pp. 877-883, 2008.

[7] Ismail, M. et al.: Effect of crack opening on the local diffusion of chloride in cracked mortar samples, Cem. Con. Res., Vol. 38, pp. 1106-1111, 2008.
[8] Sahmaran, M. and Li, V. C.: Influence of microcracking on water absorption and sorptivity of ECC, Mat. Struc., Vol. 42, pp. 593-603, 2009.
[9] Wang K. et al.: Permeability study of cracked concrete, Cem. Con. Res., Vol. 27, pp. 381-393, 1997.
[10] Zhou, C. and Li, K.: Transport properties of concrete altered by crack-induced damage, J. Mater. Civ. Eng., Vol. 27, A4014001, 2015.
[11] Choinska, M. et al.: Effects and interactions of temperature and stress-level related damage on permeability of concrete, Cem. Con. Res., Vol. 37, pp. 79-88, 2007.
[12] Aldea, C.-M., Shah, S. P. and Karr, A.: Effect of cracking on water and chloride permeability of concrete, J. Mater. Civ. Eng., Vol. 11, pp. 181-187, 1999.
[13] Rastiello, G. et al.: Real-time permeability evolution of a localized crack in concrete under loading, Cem. Con. Res., Vol. 56, pp. 20-28, 2014.
[14] Wu, Wong, H. S. and Buenfeld, N. R.: Influence of drying-induced microcracking and related size effects on mass transport properties of concrete, Cem. Con. Res., Vol. 68, pp. 35-48, 2015
[15] Multon, S. : Evaluation expérimentale et théorique des effets mécaniques de l'alcali-réaction sur des structures modèles, Université de Marne la Vallée, 2003 (in French).
[16] Kawabata, Y. et al., Correlation between laboratory and field expansion of concrete – Prediction based on modified concrete expansion test, Proceedings of 15th International Conference on Alkali Aggregate Reaction, this conference.
[17] Lindgård, J. et al..: The EU "PARTNER" Project — European standard tests to prevent alkali reactions in aggregate, Cement and Concrete Research, Vol. 40, pp.611-635, 2010.
[18] Larive, C.: Apports Combinés de l'Expérimentation et de la Modélisation à la Compréhension de l'Alcali Reaction et de ses Effets Mécaniques, Laboratoire Central des Ponts et Chaussées, OA28, 1998 (in French).
[19] Brunetaud, X., Divet, L., and Damidot, D.: Delayed ettringite formation: Suggestion of a global mechanism in order to link previous hypotheses, Proceedings of 7th CANMET/ACI International Conference on Recent Advances in Concrete Technology, pp. 63-76, 2004.
[20] Poyet, S.: Etude de la dégradation des ouvrages en béton atteints par la réaction alcali-silice : approche expérimentale et modélisation numérique multi-échelles des dégradations dans un environnement hydro-chemo-mécanique variable, PhD. Thesis of Université de Marne la Vallée, 2003 (in French).
[21] Poyet, S. et al.: Influence of water on alkali-silica reaction: Experimental study and numerical simulations, Journal of Materials in Civil Engineering, Vol. 18, pp. 588-596, 2006.
[22] Bazant, Z. P. and Najjar, L. J.: Nonlinear water diffusion in nonsaturated concrete, Mat. Struc. Vol. 5, pp. 3-20, 1972.
[23] Baghdadi, N.: Modélisation du couplage chemico-mecanique d'un béton atteint d'une réaction sulfatique interne, Ecole nationale des ponts et chaussées, 2008.
[24] Granger, L. : Comportement différé du béton dans les enceintes de centrales nucléaires : analyse et modélisation, Ecole Nationale des Ponts et Chaussées, 1995.
[25] Torrenti, J.-M. et al.: Modeling concrete shrinkage under various ambient conditions, ACI Mat. J., 96 (1999) 35-39.
[26] LCPC. Aide à la gestion des ouvrages atteints de réaction de gonflement interne.Guide technique, Laboratoire Central des Ponts et Chaussées, Paris, 2003.
[27] Multon, S., Seignol, J. -F. and Toutlemonde, F.: Structural behavior of concrete beams affected by alkali-silica reaction, ACI Materials Journal, Vol. 102, pp. 67-76, 2003.

TABLE 1: Parameter settings.

| Equations | Parameter | Value | Equations | Parameter | Value |
|---|---|---|---|---|---|
| ISR expansion (Eq. (2) for ASR expansion) | $\varepsilon_\infty$ | 1.00% | Moisture effect (Eqs. (3) & (4)) | $s_\infty$ | 0.8 |
| | $\tau_C$ | 20 days | | $m$ | 1 |
| | $\tau_L$ | 50 days | Transfer properties evolution (Eq. (7)) | $d_{max}$ | 100 |
| Moisture diffusion (Eq. (6)) | $D_0$ | 75 | | $\omega$ | 0-2 (see TABLE 2) |
| | $a_0$ | 0.075 | | $\varepsilon_{th}$ | 0-0.5 (see TABLE 2) |
| | $n$ | 6 | Shrinkage (Eq.(8)) | $k_{sh}$ | 0.0023 |
| | $s_c$ | 0.85 | | | |

TABLE 2: Calculation cases.

| | Boundary condition | Evolution of transfer evolution | $\omega$ | $\varepsilon_{th}$ | $S_{ini}$ | Remarks |
|---|---|---|---|---|---|---|
| Case 1 | constant (100%) | No | - | | 0.8 | |
| Case 2 | | Yes | 0.2 | 0.04% | | effect of $\omega$ |
| Case 3 | | | 1 | | | |
| Case 4 | | | 2 | | | |
| Case 5 | | | 1 | 0% | | effect of $\varepsilon_{th}$ |
| Case 6 | | | 1 | 0.10% | | |
| Case 7 | | | 1 | 0.20% | | |
| Case 8 | stepwise wetting (80-100%) | No | - | | 0.8 | effect of boundary conditions (wetting) |
| Case 9 | | Yes | 0.2 | 0.04% | | |
| Case 10 | | | 1 | | | |
| Case 11 | | | 2 | | | |
| Case 12 | drying/wetting (60-100%) | No | - | | | effect of boundary conditions (wetting/drying) |
| Case 13 | | Yes | 0.2 | 0.04% | | |
| Case 14 | | | 1 | | | |
| Case 15 | | | 2 | | | |

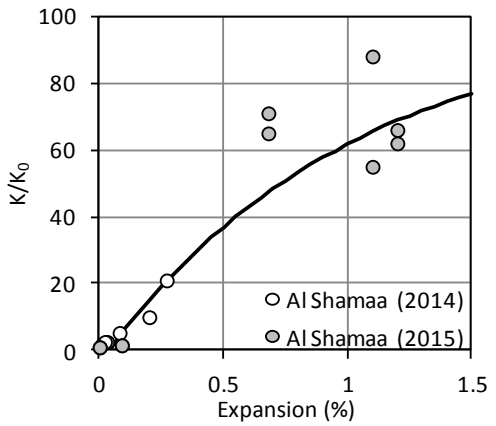


FIGURE 1: ISR expansion vs. $K/K_0$ (K: permeability, $K_0$: permeability of non-expanded concrete).

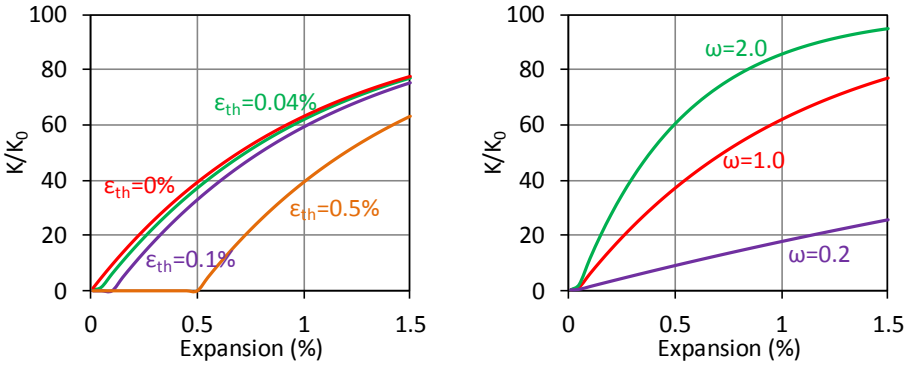


(a) $\varepsilon_{th}$ (b) $\omega$

FIGURE 2: Parameter settings for $\varepsilon_{th}$ and $\omega$ (*a. …; b. …*).

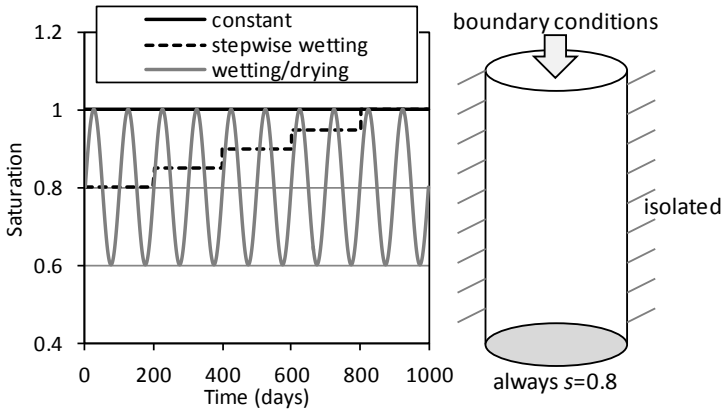


(a) three boundary conditions (b) schematic illustration

FIGURE 3: Three boundary conditions.

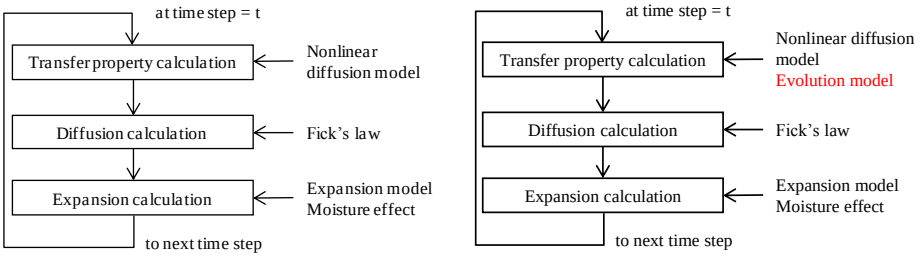


(a) Model A (without coupling) (b) Model B (with coupling)

FIGURE 4: Calculation procedures.

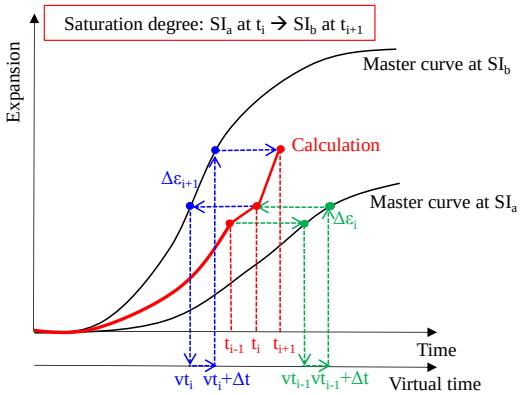


FIGURE 5: Schematic image of calculating incremental expansion at each time step.

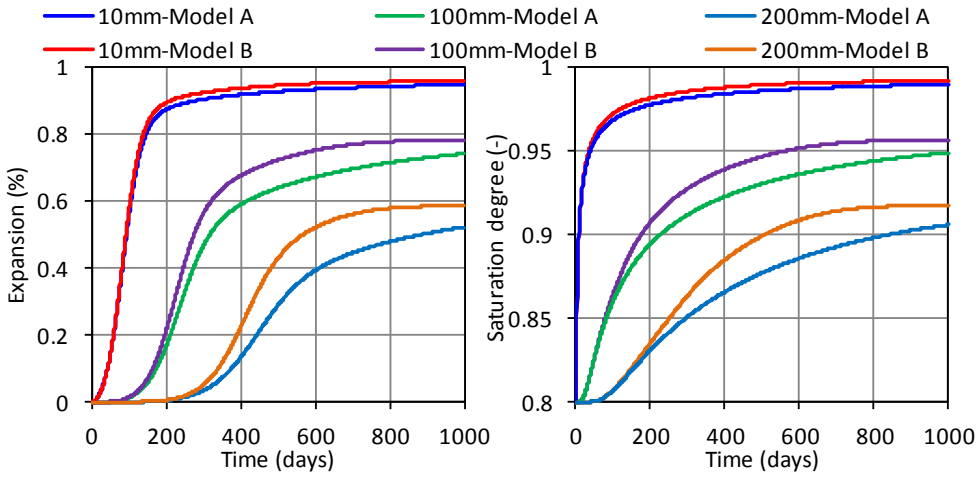


(a) constant

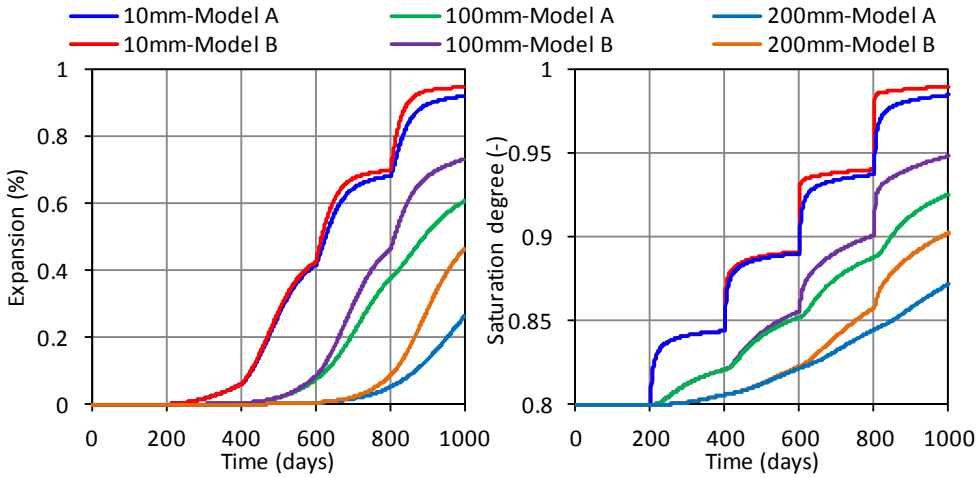


(b) stepwise wetting

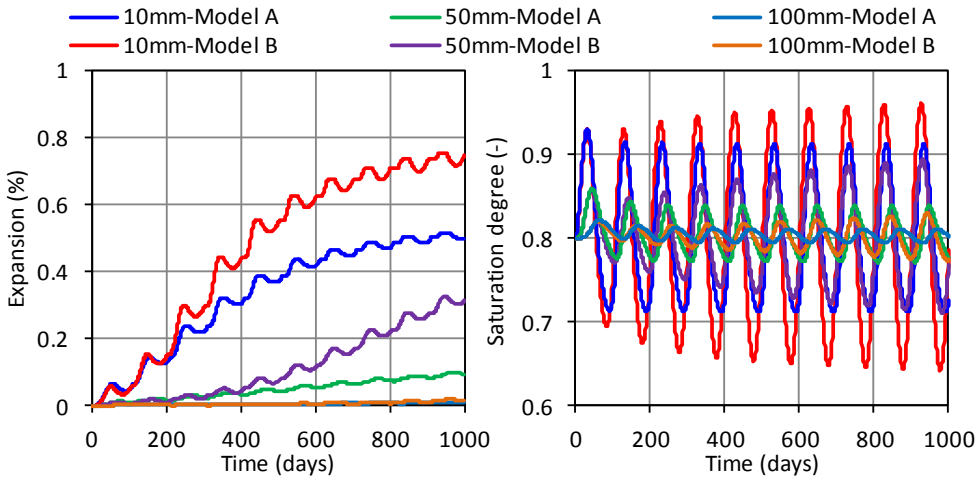


(c) wetting/drying

FIGURE 6: Simulated results of expansion and saturation degree with different boundary conditions (length correspond to the distance from the bottom of the 500 mm cylinder, Model A: without coupling, Model B: with coupling).

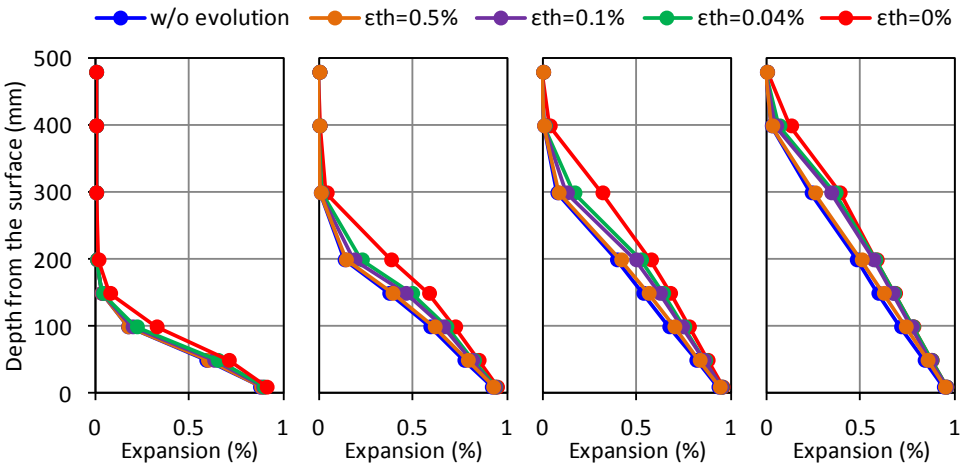


(a) 200 days (b) 400 days (c) 600 days (d) 800 days

FIGURE 7: Effect of threshold of expansion for evolution.

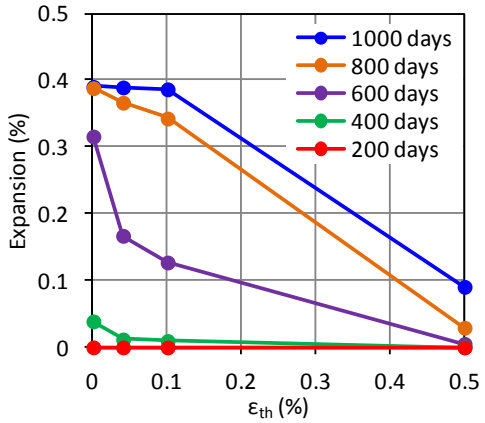


FIGURE 8: Threshold vs. expansion at 300 mm.

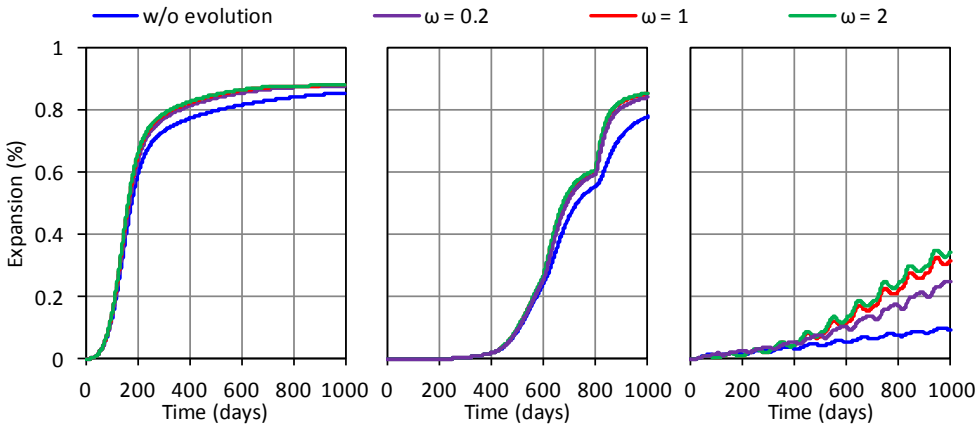


(a) constant (b) stepwise wetting (c) wetting/drying cycles

FIGURE 9: Effect of rate of evolution (50mm from the surface).